New insights into La Pacana caldera inner structure based on a gravimetric study (central Andes, Chile)

*Francisco Delgado[1, 2, 3], Andrés Pavez[2, 3, 4]

[1] *Currently at Department of Earth and Atmospheric Sciences, Cornell University, 112 Hollister Drive, Ithaca, New York, USA.*
fjd49@cornell.edu

[2] *Centro de Excelencia en Geotermia Andina (CEGA), Departamento de Geología, Universidad de Chile, Plaza Ercilla 803, casilla 13518, Correo 21, Santiago, Chile.*

[3] *Departamento de Geofísica, Facultad de Ciencias Físicas y Matemáticas, Universidad de Chile, Blanco Encalada 2002, casilla 8370449, Santiago, Chile.*

[4] *Currently at QPX Exploration, Avda. Costanera Sur 2730, Tower B, Office 701, Parque Titanium Bldg., Las Condes, Santiago.*
pavez.andres@gmail.com

* Corresponding autor: fjd49@cornell.edu

ABSTRACT. La Pacana (central Andes, Northern Chile) is one of the largest resurgent calderas in the world, formed 4 Ma ago during an eruption with a VEI of 8.7. We undertake a gravimetric study to contribute new insights into the inner structure and evolution of this caldera. The La Pacana Bouguer residual anomaly is asymmetric and has an average amplitude of -12 to -14 mGal, which we interpret as being produced by the low-density intracaldera ignimbrite infill. A reinterpretation of the caldera stratigraphy plus the available geochronology suggests that the current shape of La Pacana was produced by the collapse of two nested calderas, roughly limited by the axis where the resurgent dome changes its orientation, with the oldest eruption in the southern part of La Pacana. The gravity data suggests that these southern and northern nested structures would have collapsed with downsag and trap-door geometries respectively, evidence of asymmetric subsidence. Intra caldera ignimbrite thicknesses were calculated with 2.5D forward models and show that the ignimbrite infill in its southern and northern parts reach ~0.6-1.1 km and ~2.5-3 km respectively. Using Gauss's theorem, we calculate the volume of the intra caldera ignimbrite infill is ~3,400-3,500 km^3, in agreement with previous estimates and with models that show that the larger the caldera diameter, the larger the erupted volume.

Keywords: La Pacana caldera, Volcanology, Gravimetry, Caldera collapse.

RESUMEN. Nuevos antecedentes sobre la estructura interna de la caldera La Pacana mediante un estudio gravimétrico (Andes centrales, Chile). La Pacana (Andes centrales, norte de Chile) es una de las calderas resurgentes más grandes del mundo, formada 4 Ma atrás en una erupción con un VEI de 8,7. Hemos realizado un estudio gravimétrico de la caldera para contribuir con nuevos antecedentes sobre su estructura interna y evolución. La anomalía residual de Bouguer de La Pacana es asimétrica y tiene una amplitud promedio de entre -12 a -14 mGal, la que se interpreta que es producida por el relleno de baja densidad de ignimbritas intracaldera. Una reinterpretación de la estratigrafía de la caldera junto con la geocronología disponible sugiere que la forma actual de La Pacana fue producida por el colapso de dos calderas anidadas, cuyo límite aproximado sería el eje donde el domo resurgente cambia su orientación, y con la erupción más antigua en la parte sur de La Pacana. Los datos gravimétricos sugieren que estas estructuras anidadas sur y norte habrían colapsado con geometrías de tipo *downsag* y *trap-door* respectivamente, evidencias de subsidencia asimétrica. Los espesores de las ignimbritas intracaldera fueron calculados con modelos directos en 2.5D los cuales muestran que el relleno en sus partes sur y norte alcanza a los ~0,6-1,1 km y ~2,5-3 km respectivamente. Mediante el teorema de Gauss, calculamos que el volumen de las ignimbritas intracaldera llega a los ~3.400-3.500 km^3, de acuerdo con estimaciones previas y con modelos que muestran que mientras más grande es el diámetro de la caldera, mayor es el volumen de material eruptado.

Palabras clave: Caldera La Pacana, Volcanología, Gravimetría, Colapso de calderas.

1. Introduction

Resurgent calderas, also known as supervolcanoes, are the result of the largest volcanic eruptions on the geological record, which have been at least two orders of magnitude bigger than any eruption ever registered by humans (*e.g.,* Newhall and Self, 1982; Mason *et al.*, 2004; Miller and Wark, 2008). The large size of these eruptions (volumes larger than 450 km^3 and a Volcanic Explosivity Index (VEI) greater than 8) has attracted a growing global interest to understand the evolution and eruptive dynamics of the biggest calderas (Wilson, 2008), by studying their emitted products and the formation of their structure and geometry (Sparks *et al.*, 2005; Acocella, 2007; Martí *et al.*, 2008; Hardy, 2008). Due to the lack of observations of eruptions of this size, the caldera dynamics and the climatic impact of these supereruptions, including the effects over the human population, are poorly understood (*e.g.*, Cole *et al.*, 2005; Lipman, 1997; Self, 2006; Jones *et al.*, 2007; Self and Blake, 2008). The largest ignimbrite flare-ups in the world (*e.g.*, Taupo volcanic zone, New Zealand; San Juan mountains, SW United States; Altiplano Puna Volcanic Complex APVC, southern central Andes of Bolivia, Chile and Argentina) are the places where the largest calderas in the world are located (Lipman, 2007; Rowland *et al.*, 2010; De Silva, 1989a; De Silva *et al.*, 2006; De Silva and Gosnold, 2007) and then constitute ideal study cases to investigate the dynamics of these supervolcanoes. The caldera inner structures are important in hazard assessment, as some of them show ground deformation likely related to magma intrusion (*e.g.*, Wicks *et al.*, 2006; Battaglia *et al.*, 1999). Since caldera inner structures are normally covered by inflow ignimbrites, geophysical data are key elements to understand them and their dynamics.

In this work, we present a gravimetric study of the inner structure of La Pacana, the largest caldera in the Altiplano Puna Volcanic Complex (*e.g.*, Gardeweg and Ramírez, 1987; De Silva, 1989a, b), which produced the fifth largest eruption ever registered in the geological record (*e.g.*, Mason *et al.*, 2004). Despite its size and importance, the existing geological studies (Gardeweg and Ramírez, 1987; Lindsay *et al.*, 2001a, b) have several discrepancies regarding caldera limits, intra caldera ignimbrite thicknesses, collapse geometries and erupted volumes. We use gravimetry because it has been successfully used in caldera studies elsewhere to measure the subsurface caldera structure and deposit thickness -potentially resolving the discrepancies in previous interpretations (*e.g.,* Rymer and Brown, 1986; Carle, 1988; Davy and Caldwell, 1998; Masturyono *et al.*, 2001; Smith *et al.*, 2006; DeNosaquo *et al.*, 2009; Seebeck *et al.*, 2009; Drenth *et al.*, 2012). Based on both a gravity model and the reinterpretation of the ignimbrite stratigraphy, we suggest that the collapse geometry is significantly different than previously proposed, and that La Pacana caldera is made up of at least two nested calderas of different ages. We also provide estimates of the erupted volume and the collapse mechanism.

2. Geological Framework

The detailed geology of La Pacana caldera has been described elsewhere (Ramírez and Gardeweg, 1982; Gardeweg and Ramírez, 1985; Gardeweg and Ramírez, 1987; Lindsay, 1999; Lindsay *et al.*, 2001a,b; Schmitt *et al.*, 2002; Gardeweg and Lindsay, 2004). Here, we focus on the geological setting, the main structural elements including the resurgent dome and the caldera rim, and the caldera stratigraphy. La Pacana is the largest caldera of the Altiplano Puna Volcanic Complex of the central Andes (APVC), the largest Neogene ignimbrite flare-up in the world, with an area of 30,000 km^2 (*e.g.*, De Silva, 1989a, b; De Silva *et al.*, 2006; De Silva and Gosnold, 2007). The APVC ignimbrite volumes are larger than 1,000 km^3 and their sources are several asymmetrical calderas that form huge depressions (*e.g.*, De Silva and Gosnold, 2007), possibly with a tectonic control (Riller *et al.*, 2001; Ramelow *et al.*, 2006). The APVC eruptive activity started 13 Ma ago (*e.g.*, Schmitt *et al.*, 2002) and occurred in short and intense eruptive pulses each ~2-3 Ma (*e.g.*, Salisbury *et al.*, 2011). However, 2 Ma ago the volcanic activity decreased in magnitude and the eruptive style shifted to smaller and more effusive eruptions (*e.g.*, De Silva and Gosnold, 2007; Salisbury *et al.*, 2011). At a much larger, whole crustal scale, the APVC structure has been studied from a geophysical point of view by seismic tomography and receiver functions (*e.g.*, Chmielowski *et al.*, 1999; Zandt *et al.*, 2003; Ward *et al.*, 2014), electromagnetic methods (Schilling *et al.*, 2006; Comeau *et al.*, 2015), and gravity (*e.g.*, Götze and Krause, 2002; Tassara *et al.*, 2006; Riller *et al.*, 2006; Del

Potro *et al*., 2013). These studies show either the possible presence of magma body about 17 km below the surface (APMB, Altiplano Puna Magma Body) and an upper crust of felsic composition.

La Pacana caldera is located in the southern part of the APVC in the Antofagasta political region of northern Chile with its center at 67°25' W and 23°10' S (Fig. 1 and 2) and is a 60 by 35 km asymmetrical

caldera elongated in the NS direction. The caldera topographic margin is well exposed in its S part and has a maximum relief up to 1,000 m above the moat (Gardeweg and Ramírez, 1987). Gardeweg and Ramírez (1987) suggested that caldera subsidence was differential with the thickest intracaldera ignimbrite in the resurgent dome and decreasing towards both the north and south. However, the exact intracal-
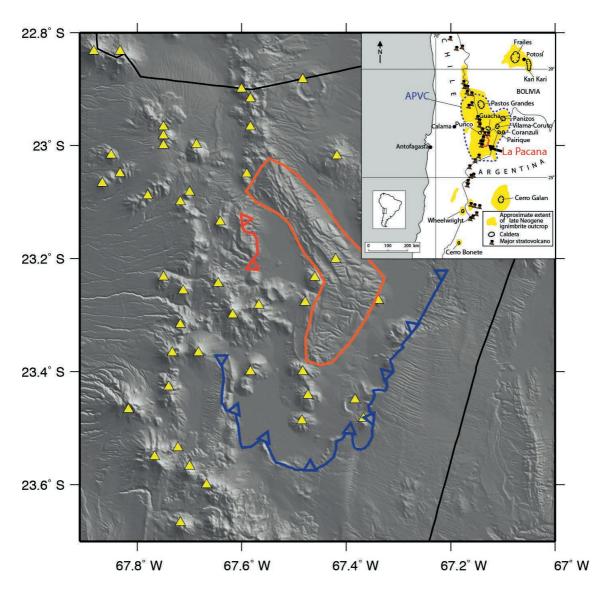

FIG. 1. Shaded SRTM topography of La Pacana caldera. The red and blue lines are the west and south caldera rims (Lindsay *et al*., 2001a). Open triangles show the caldera hanging wall, the orange line is Cordón La Pacana resurgent dome boundary, the red triangles are Miocene-Holocene volcanic centers (Ramírez and Gardeweg, 1982; Gardeweg and Ramírez, 1985; Lindsay *et al*., 2001a) and the black line is the Argentina-Bolivia-Chile border. Inset (colored from Lindsay *et al*., 2001a) shows the location of La Pacana caldera within the Altiplano Puna Volcanic Complex (APVC) in the central Andes.
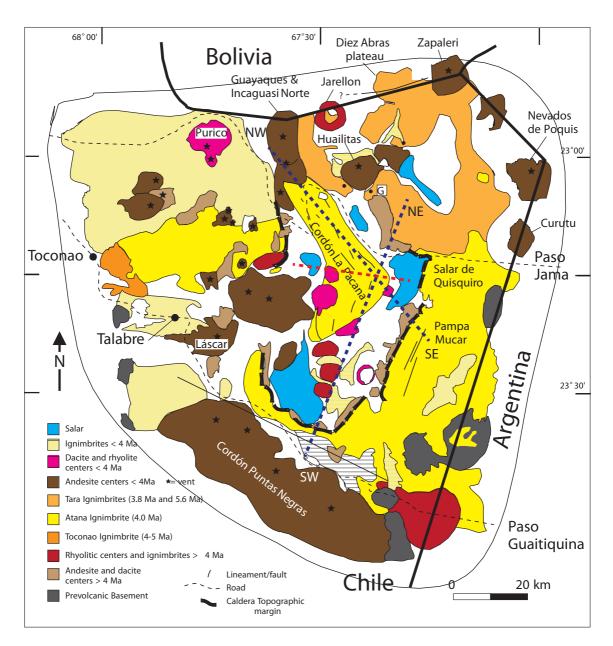
FIG. 2. La Pacana caldera geological map (Lindsay *et al*., 2001a; Gardeweg and Lindsay, 2004). The rhyolitic centers within the southern part of the caldera moat (red bodies south of Cordón La Pacana) have been modified from the original map. Dashed blue lines and text labeled as NW, NE, SE and SW are the trace of the modeled cross sections in figures 4 and 5, and the dashed red line shows the inferred limit between the southern and northern caldera collapses (see discussion section).

dera ignimbrite thickness is unknown, as its base is not exposed. They proposed that the intra caldera ignimbrite maximum thickness is 0.9 km near the resurgent dome. Unlike the above mentioned study, the lack of a topographic margin in the N part of La Pacana led Lindsay *et al*. (2001a) to propose that the

collapse mechanism was a trap-door geometry with a hinge region near the northern edge of the mapped caldera. These authors assumed a minimum thickness of intracaldera ignimbrite of 2 km for La Pacana as a whole, which would be thicker in the southern part of the caldera, an infill discrepancy of more than

1 km with respect to Gardeweg and Ramírez (1987) estimate.

For the most part, La Pacana overlies a sequence of late Miocene pre caldera ignimbrites and volcanic rocks, and locally, upper Paleozoic volcanic and lower Paleozoic sedimentary basement (Ramírez and Gardeweg, 1982; Gardeweg and Ramírez, 1985; Gardeweg and Ramírez, 1987; Bahlburg *et al*., 1988; Breitkreuz and Zeil, 1994; Lindsay *et al*., 2001a) (Fig. 2). Due to the complexity of the caldera and the lack of dissection, the La Pacana collapse has been proposed to be produced by the eruptions of either Atana (4.11-4 Ma) (Gardeweg and Ramírez, 1987), Atana and Toconao (4.65 Ma) (Lindsay *et al*., 2001a,b; Schmitt *et al*., 2002), Pujsa (5.7 Ma) and Atana (Pavez *et al*., 2008) ignimbrites, or all of them (De Silva and Gosnold, 2007) (Fig. 2). Regardless of the erupted ignimbrites, the eruptions resulted in ponding of these units within the collapse area into a thick sequence of intracaldera ignimbrite and a smaller outflow volume. Some of the ignimbrites inside the caldera might have been erupted from other calderas in the area (Lindsay *et al*., 2001a). Post-eruption resurgence of La Pacana led to the formation of an uplifted asymmetric elongated dome of intracaldera tuff known as Cordón La Pacana. This dome occupies 24% of the area within the topographic depression with long and short axis of maximum lengths of 48.5 and 12 km trending in the NW-SE and NE-SW directions respectively (Fig. 1), with its highest part reaching ~5,200 m above sea level, almost 1 km above the caldera moat lying at ~4,200-4,500 m. The dome is broken by several NW-SE and SW-NE striking normal faults produced by its resurgence (Gardeweg and Ramírez, 1987). This asymmetrical geometry and a reinterpretation of the domes that intrude the southern part of the resurgent dome (Arenoso, Chivato Muerto, and Chamaca domes, red bodies in the caldera moat in figure 2, syn-caldera domes hereafter) and their available K-Ar ages (Gardeweg and Ramírez, 1987; Lindsay *et al*., 2001a) led Pavez *et al*., (2008) to propose that La Pacana could be at least two nested calderas (the inferred limit is the dashed red line in figure 2) produced by two major eruptive events (see discussion for further details). Finally, post caldera volcanism lasted from 4 up to 2 Ma (Gardeweg and Ramírez, 1987; Lindsay *et al*., 2001a) and occurred as dacitic dome and stratovolcanoes extrusions along the western,

southern, and eastern edges of the resurgent dome (Lindsay, 1999).

3. Data Acquisition and Processing

71 gravity stations were acquired in a survey in January-February 2009 with a LaCoste & Romberg G411 gravity meter and a pair of Leica SR20 single frequency geodetic receivers with Leica AT501 antennas. Due to the large distances in the survey area, the gravity base station was measured at the beginning and the end of the daily surveys and several cross-loops were measured using relative stations tied to the reference benchmark. Additional observations were provided by 20 stations acquired by Pavez (2005) and 647 gravity stations acquired between 1,982 and 1,994 from the central Andes gravity data base (Schmidt and Götze, 2006). Due to its pre GPS date, the elevation benchmark of each station of the latter database had to be validated before it was merged with the newest data.

The dataset was reduced using standard procedures (Telford *et al*., 1990; Blakely, 1996). The earth tide was corrected with Longman's formula (1959), while the drift correction was calculated with the CGxTOOL software (Gabalda *et al*., 2003). Resulting drifts were lower than 0.3 mGal/day, in agreement with literature (Blakely, 1996). The 2009 data set was tied to the central Andes database, which is part of the IGSN71 gravity net (Morelli *et al*., 1974). On the other hand, GPS benchmarks were tied to the Caltech Chajnantor (CJNT) continuous geodetic station (Simons *et al*., 2010). The GPS bases for each day of the survey were then processed in the Spectra Precision Survey Office software in static mode tied to CJNT, decimating the data to the common sampling rate of 0.033 Hz. Then, the GPS rover of each gravity station was processed in kinematic or fast static mode tied to its daily GPS base. Baselines were shorter than 25 km and measurement times of each GPS station were 7 minutes on average, yielding a vertical accuracy of less than 1 m for the 2009 data. As an example, for 3 and 25 km GPS base lines, horizontal accuracy was less than 0.3 and 0.8 m respectively. Due to the lack of dual frequency GPS positioning of the central Andes gravity data base, the stations where repositioned with pre existent kinematic GPS tracks and their elevations were recalculated using the 3 arcsec Shuttle Radar Topographic Mission (SRTM)

digital elevation model (DEM) (Farr *et al*., 2007). This DEM has a spatial resolution of 90 m/pixel and was leveled by adding the difference between this data set and the elevation of all the geodetic GPS stations and tracks (35 m), and then used to extract the elevation benchmarks of the latter gravity database.

The accuracy of the different gravity data sets is variable. The Lascar volcano gravity data (Pavez, 2005) accuracy is better than 0.05 mGal, while the accuracy of the 2009 survey varies between 0.05 and 0.1 mGal. The accuracy of the elevation benchmarks of the gravity stations can be compared converting the former figures to the free air gradient of 0.3086 mGal/m. This means that the elevation benchmarks of the 2009 data are better than 0.25 mGal, which are the expected uncertainties in a regional survey like this. Hence the combined 2002-2009 data accuracy is better than 0.22 mGal. Schmidt and Götze (2006) data are not as accurate as the former because the difference between the GPS and SRTM elevation benchmarks has a standard deviation of 13 m, therefore the gravity related error is 4 mGal of free air correction, still an acceptable figure for this regional work.

The Bouguer residual anomaly separates anomalies produced by bodies not accounted for by a simple density reference model of the crust and was calculated with standard expressions (Moritz, 1984; LaFehr, 1991a; Blakely, 1996), implemented in the Geosoft Oasis montaj software. The topographic correction was calculated with the SRTM DEM using standard algorithms (Nagy, 1966; Hammer, 1939; Kane, 1962) and the Bouguer correction included the Bullard B correction (LaFehr, 1991b) to account for the Earth's curvature. The terrain density for the Bouguer correction is one of the most critical parameters in gravity reduction because the resulting anomalies can be over or underrepresented depending on the density contrast, especially when the lithological variations are large such as the study areas with multiple ignimbrites and facies. On the other hand, the non-uniqueness separation of the regional/residual field associated to long-wavelength-deep-seated-bodies/shorth-wavelength-shallow-geological-features, can also lead to over or underrepresentation of geological anomalies (*e.g*., Gupta and Ramani, 1980; Simpson *et al*., 1986; Blakely, 1996). A simple form to calculate a reasonable density and isostatic model is to minimize the Bouguer residual anomaly by linear least squares, to reduce its correlation with the topography (Nettleton, 1939; Parasnis, 1962; Torge, 1989) a method used in volcanic studies elsewhere (*e.g.*, Tiede *et al*., 2005; Pavez, 2005). The inverted density is 2.2 g/cm^3, which is a reasonable value for a lowdensity ignimbrite covered area. The resulting Bouguer residual anomaly was finally gridded with the minimum curvature algorithm (Briggs, 1974) with a cell size of 3 km.

4. Results

4.1. Bouguer residual anomaly

The Bouguer residual anomaly shows a strong and asymmetrical NS elongated negative anomaly (shades of green and blue in figure 3) which is broader than La Pacana caldera boundaries, with an average amplitude of -12 to -14 mGal reaching -21 and -40 mGal in the southern and northern parts of the caldera respectively, the global minimum located in the northern part of the resurgent dome (Fig. 3). This signal is surrounded by strong positive anomalies with maximum amplitudes of 30 and 45 mGal west and east of La Pacana. All of these signals have amplitudes at least 3 to 9 times above the error level. Different interpretations on the origin of the low density-negative gravity anomaly have been proposed including the APMB or a batholith (De Silva *et al*., 2006), brittle felsic upper crustal rocks (Riller *et al*., 2006) or low-density ascending diapiric bodies rooted in the APMB in the northern part of the APVC (del Potro *et al*., 2013). However, as the observed negative anomalies are spatially related with La Pacana caldera, we consider that the most likely source of this signal is the low-density intracaldera ignimbrite facies, in agreement with studies in caldera environments elsewhere (*e.g*., Rymer and Brown, 1986; Carle, 1988; Masturyono *et al*., 2001). On the other hand, relative positive anomalies such as the signal in the middle of the caldera and spatially related with volcanic edifices (Fig. 3) are interpreted as being produced by dense intrusive bodies (*e.g*., Rymer and Brown, 1986; Malengreau *et al*, 1999; Gudmundsson and Högnadóttir, 2007), due to the crystallization of the densest mineralogical phases during magma ascent and emplacement. Finally, positive anomalies outside of the caldera are interpreted as the response to the uplift of dense Paleozoic basement.
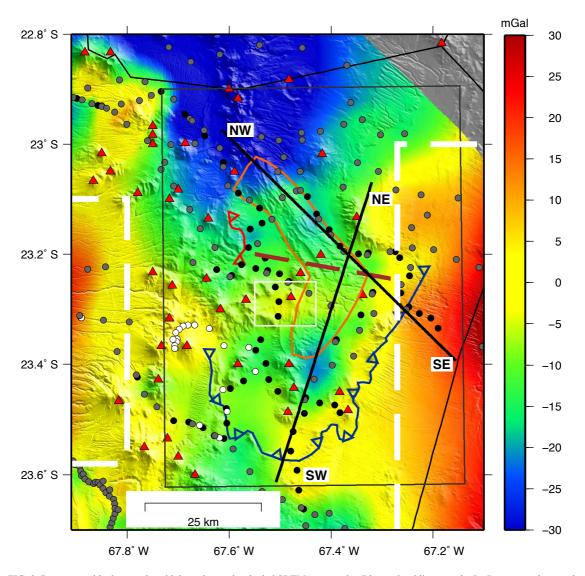
FIG. 3. Bouguer residual anomaly grid draped over the shaded SRTM topography. Blue and red lines are the La Pacana southern and western rim (Lindsay *et al*., 2001a). Open triangles show the caldera hanging wall. The dashed brown line is the inferred border between the N and S parts of La Pacana. Black, white and grey circles are gravity stations acquired in the 2009 summer, by Pavez (2005) and Schmidt and Götze (2006). Red triangles are Miocene-Holocene volcanic centers (Ramírez and Gardeweg, 1982; Gardeweg and Ramírez, 1985; Lindsay *et al*., 2001a). White dashed lines delimit positive anomalies interpreted as being produced by Paleozoic basement. White box is an example of a relative positive anomaly interpreted as being produced by intrusive bodies beneath the volcanic edifices. Black lines indicate the selected profiles where gravity forward modeling was carried out. White letters indicate the directions of the forward models in figures 4 and 5. The grey box is the extent of the grid used in the calculation of the intra caldera mass deficit**.**

4.2. 2.5D Forward Modeling

In order to quantify the Bouguer residual anomaly interpretation, we calculated 2.5D forward models along two transects. These sections allow an estimate of the intracaldera infill thickness, margin geometry, and geometry of the underlying bodies. These profiles (black lines in figure 3) were chosen to traverse gravity anomalies of geological interest in places where the contribution to the gravity field is mostly associated with the newer gravity data, ensuring that uncertainties are below 1 mGal. The forward

modeling was carried out in the software ENCOM ModelVision Pro, based on the Talwani's algorithm implemented by Cady (1980) for the case of 2.5D bodies of limited extension and symmetric in the third coordinate and with different densities. The densities of the modeled bodies were measured from field samples, and in the case of intrusive bodies, extrapolated from dome densities (Table 1). The polygon shapes were constrained with geological information when available, such as mapped caldera structures or borehole data. In order to reduce the strong non-uniqueness of the forward models (*e.g.*, Roy, 1962), intrusive bodies shapes are kept as simple as possible, thus simple shapes such as ellipsoids approximated some of them. Therefore, we consider the modeled geometries a simplified model of the real caldera structure. Based on the arguments of the previous section, we make the assumption that the negative gravity signal is produced by low-density intracaldera infill and that the underlying basement has no density contrast with respect to the density reference model. Finally, we state that there are minor differences of 100-200 m in the thickness of the modeled bodies at the intersection points of the profiles, which are produced by considering the 3D caldera structure as 2.5D, which do not change the overall interpretations of this work.

4.3. SW-NE Cross Section

This section (Fig. 4) traverses the southern part of La Pacana caldera, where the gravity signal reaches up to -21 mGal, thus the deepest area of this section of La Pacana. The gravity anomalies are always negative, but reach relative maximums within the caldera moat (-2 mGal) and in the post caldera volcanoes (-7 mGal), while the minimum values are below the resurgent dome. The profile is modeled with five bodies, two with positive densities

TABLE 1. DENSITIES USED IN THE GRAVITY FORWARD MODELS (FROM PAVEZ, 2005).

Geological Unit	Density (g/cm³)
Ignimbrites	1.8-2.0
Intrusive bodies	2.5-2.8
Mesozoic basement	2.1-2.2
Paleozoic basement	2.4-2.6

interpreted as shallow intrusive bodies feeding domes and stratovolcanoes, the third with a negative density contrast interpreted as La Pacana intracaldera ignimbrite infill, and two with negative density contrast required to fit the gravity signal outside of the caldera and interpreted as undifferentiated low density ignimbrites. The intracaldera thicknesses are variable, with a minimum of 0,6 km below the caldera moat and a maximum of 1,1 km in its deepest part below the resurgent dome with some fluctuations in between (Fig. 4). The possible collapse geometries (Lipman, 1997; Cole *et al*., 2005) arising from the modeled ignimbrite infill are described in the discussion section. We speculate that the intracaldera ignimbrite infill in the southern part of the caldera is made up of several ignimbrites besides Atana (see discussion section), but due to the lack of density contrast we can not determine the boundary between the different volcanic deposits in the gravity model. The ignimbrite infill is modeled with respect to the described topographic margin, limited by normal faults according to analog models (Acocella, 2007; Hardy, 2008; Martí *et al*., 2008) and with their sense of slip inferred from these models (Fig. 4), therefore more complex structures such as the caldera collapse collar (Lipman, 1997) are not taken into account Although andersonian normal faults are expected to dip ∼60°, the modeled dips are shallower and steeper along the interpreted structure. Finally, the forward model shows that the roof of shallow intrusive bodies is located at ∼1.5-2 km below the surface and the ignimbrite sheets. These intrusions are broader in wavelength than the fed syn-caldera domes and post caldera stratovolcanoes, and given their densities they are most likely of dacitic composition. Due to the strong non-uniqueness in gravity forward models and the lack of further constraining data, we have assumed that the material between the domes and the intracaldera infill does not have a density contrast with respect to the density used in the Bouguer residual anomaly calculation.

4.4. NW-SE Cross Section

The second cross section (Fig. 5) was chosen to traverse the northern part of La Pacana through the caldera moat and the resurgent dome. The gravity anomaly decreases from 18 mGal in the SE part, to -30 mGal in the NW, with some fluctuations in between. Three bodies were considered to fit the
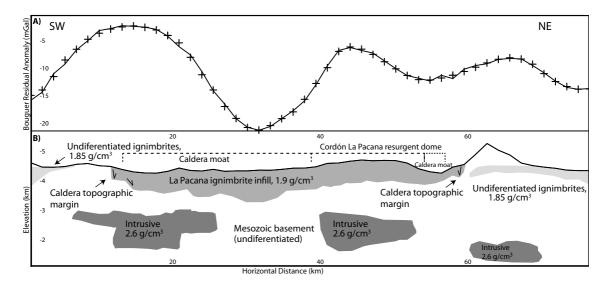
FIG. 4. Forward model of the SW-NE cross section. **A.** Bouguer residual anomaly (crosses) and model prediction (continuous line); **B.** Topography (negative above sea level) and model geometry. Numbers are the densities used in the forward modeling. Arrows in the intracaldera infill are interpreted as normal faults in the caldera hanging wall. Dashed lines delimit the caldera moat and resurgent dome. See text for details.
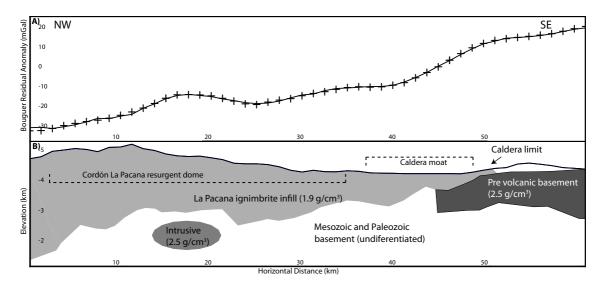

FIG. 5. Forward model of the NW-SE cross section. Legend as in figure 4.

gravity signal, which account for the intracaldera infill, an intrusive beneath the resurgent dome and the pre-volcanic basement. Unlike the previous section, we model part of the pre-volcanic basement as it outcrops east of La Pacana (Gardeweg and Ramírez, 1985) and the gravity signal of the uplifted basement is required to fit the data. The modeled

ignimbrite thickness increases towards the NW reaching a maximum of ~2.5-3 km, but the NW limit of the ignimbrite infill cannot be properly determined with the limited data set. The intrusive body below the resurgent dome produces the local maximum in the gravity signal as a result of being located close to the highest part of the resurgent dome; hence its

emplacement could have been responsible for the dome uplift as shown by overpressure analogue experiments (Acocella, 2007).

5. Discussion

5.1. La Pacana caldera depth infill estimates and limits: evidence for the presence of nested calderas

The modeled intracaldera infill thickness is validated with borehole data in the southern part of the caldera moat (M. Gardeweg, personal communication, 2009) on which the pre volcanic basement lies 0.6 km below the surface. Thus, the ignimbrite infill in this area has a maximum depth of 1.1 km in the resurgent dome and decreases towards the southern part of La Pacana (Fig. 4), while the ignimbrite infill reaches 2.5-3 km in its NW part (Fig. 5). The former ignimbrite model is more akin to the 1 km of intracaldera infill that Gardeweg and Ramírez (1987) proposed for the central part of the caldera than the 2 km assumed by Lindsay *et al*. (2001a). The caldera northern boundary cannot be properly delimited with the available data set as the large scale negative gravity signal (Fig. 3) does not show clear boundaries and is not well constrained by the newer gravity data set.

A reinterpretation of the La Pacana available stratigraphy and geochronology lead us to consider a different origin for the modeled intracaldera ignimbrites than the inferred interpretations arising from Gardeweg and Ramírez (1987) and Lindsay *et al*. (2001a). The southern part of Cordón La Pacana dome is intruded by three syn-caldera domes (red units within the caldera moat in figure 2), for which only a single age K-Ar age of 4.8+0.2 Ma is available (Gardeweg and Ramírez, 1985, 1987) that lead these authors to suggest that these units are pre-caldera collapse as they are older than the Atana ignimbrite. However, Lindsay *et al*. (2001a) pointed out that as they lie over the southern part of the resurgent dome, they must be younger than the latter unit. The age of these syn-caldera domes overlaps with the only Atana ignimbrite K-Ar age for the southern part of the resurgent dome of 4.5+0.4 Ma (Gardeweg and Ramírez, 1987). But most of the available Atana K-Ar ages are younger and span ranges between 4.2 and 3.7 Ma with an average of 4.0 Ma (Gardeweg and Ramírez, 1987; De Silva, 1989b; Lindsay *et al*., 2001a), while its U-Pb ages are

4.11+0.2 Ma (Schmitt *et al*., 2002) therefore we consider the 3.7-4.2 Ma time span as the most representative Atana age. This implies either the syn-caldera domes were intruded into the resurgent dome quickly after the emplacement of the latter or as they lie within the caldera moat, they are older than the resurgent dome in the southern part of La Pacana caldera. As the accepted ages for the eruption of the Atana ignimbrite are younger than the syn-caldera domes, we suggest that the southern part of La Pacana was produced by an older eruption and collapse than the Atana eruption that generated its northern part as older volcanic edifices do not intrude the resurgent dome in this area (Ramírez and Gardeweg, 1982; Gardeweg and Ramírez, 1985), Hence, the observed caldera geometry would be the result of a nested collapse, whose limit is inferred to be roughly the zone where the resurgent dome changes its orientation from NW-SE to NE-SW (brown dashed line in figures 2 and 3). Therefore most of the intracaldera infill modeled in figure 4 is made up of Atana and older ignimbrites, but we cannot assess with the available data whether any of the pre-Atana ignimbrites like Toconao (Fig. 2) were erupted from this area. We acknowledge that this interpretation is highly speculative as it is based in single K-Ar ages for each of the geological units and the low spatial resolution of the gravity data set. The lack of density contrast between the ignimbrites hampers the ability to calculate gravity gradients that could be used to determine density boundaries between the two nested calderas. In the absence of more observations and data, we have not attempted to further redefine the caldera limits besides the first order observation that the boundary may be where the resurgent dome changes strike. On the other hand, elliptical calderas have been proposed to be elongated parallel to the minimum horizontal stress (Holohan *et al*., 2005), in agreement with regional tectonics that show an horizontal σ_1 of west-east direction during the Pliocene (González *et al*., 2009). However, La Pacana elliptical shape could also be produced by the nested collapse of the smaller calderas, which hampers the assessment of whether the caldera set final shape is tectonically controlled or not.

5.2. Collapse mechanisms and geometry

The different gravity signals inside La Pacana caldera provide new insights about the caldera collapse mechanism and geometry. The superposition of the

intrusive gravity signals inside La Pacana complicates the interpretation of the collapse geometry as the Bouguer residual anomaly is produced by multiply bodies; hence our data can not be used to support complex collapse geometries such as a piece-meal model in which several blocks fall asymmetrically during the caldera collapse. Gardeweg and Ramírez (1987) suggested a central ring fault around the resurgent dome, while Lindsay *et al.* (2001a) noted the lack of a northern topographic border and proposed a trap-door geometry with a northern hinge zone. Based on the previous section, we assume that the caldera is made up of two different collapses, hereafter PS (Pacana south) and PN (Pacana north). The presence of a negative anomaly close to PS central part (Fig. 3) suggests a downsag collapse geometry (Cole *et al.*, 2005), with maximum subsidence near the caldera center. Compared with the earlier Gardeweg and Ramírez (1987) and Lindsay *et al.* (2001a) proposals, our model for PS caldera is more consistent with the former. On the other hand, as the forward model (Fig. 4) shows that the gravity signal is deeper towards PN northwest zone, we suggest a trap-door mechanism for this caldera with a hinge zone in the area where the resurgent dome changes its orientation (brown line in figure 3).

5.3. Mass deficit and erupted volume (VEI)

One of the key parameters in all caldera studies is the volume of the ignimbrite infill and outflow, which allows to estimate the VEI of the associated eruptions (*e.g.*, Miller and Wark, 2008). The volume estimation of old eruptions as in the APVC is a nontrivial task due to the lack of dissection that hampers estimation of the ignimbrites' thicknesses and the petrological similarity of ignimbrites erupted from different calderas. This calculation is based on simple assumptions such that the intracaldera and outflow volume deposits are approximately equal; therefore the volumes are only order of magnitude estimates (*e.g.*, Mason *et al.*, 2004). These assumptions do not hold for the APVC calderas (Salisbury *et al.*, 2011). For La Pacana caldera, the previous work has presented different erupted volumes, based on the assumption of different geometries for the caldera inner structure (Lipman, 1997). Gardeweg and Ramírez (1987) estimated the erupted volume to be ~900 km³, while Lindsay *et al.* (2001a) estimated ~2,500 km³. Unlike the previous studies, we propose to use Gauss's

theorem to calculate the mass deficit produced by the caldera eruptions and the associated volume, which has been used in other calderas (Campos-Enríquez *et al.*, 2005). According to Gauss's theorem (*e.g.*, Hammer, 1945; LaFehr, 1965), the mass M related to a gravity anomaly Δg measured over the Earth's surface (S) is

$$\Delta M = \frac{1}{2G} \iint_{X-Y} (\Delta g) dS$$

with G the gravitational constant ($6.67*10^{-11}$ Nm²/kg). This formula is discretized for cells with constant area S as

$$\Delta M = \frac{S}{2G} \sum_i g_i$$

where g_i is the gravity anomaly of the i grid cell. The main advantage of Gauss's theorem is that the mass estimate is independent of the anomalous body geometry. Therefore, any VEI calculated with the combined mass of the coeruptive ignimbrites must be regarded as a total value that cannot discriminate different eruptions. However, it posses some disadvantages, such as a proper regional, residual gravity fields separation, which could over or underrepresent the mass related to the gravity anomalies. Another disadvantage is that the exact surface that contains La Pacana caldera is not regular, so if the calculation is carried out with a square grid, the resulting mass deficit figure has to be reduced to take into account an estimate of the percentage of cells that do not contain the caldera gravity signal. The only way to improve this procedure (and beyond the scope of this paper) is to calculate a 3D model of the caldera structure and estimate the mass directly from the volume of the modeled polyhedrons.

The gravity grid used to calculate the mass deficit is shown within the grey box in figure 3. As part of the gravity signal of the ignimbrites is outside the caldera, the box extends some distance from the caldera topographic margin. The calculated mass deficit of La Pacana is $-1.08*10^{15}$ kg, but as the grid is bigger than the caldera extent, the previous figure has to be reduced 20%, with a resulting mass deficit of $-8.6*10^{14}$ kg. We calculate the volume with the same density contrast of -300 kg/m³ that was used in the caldera intracaldera forward models, with a resulting ignimbrite infill of 2,868 km³. The outflow

volume has been estimated between 240 (Gardeweg and Ramírez, 1987) and 270 km³ (Lindsay *et al.*, 2001a), so we assume an average of 255 km³. An additional outflow is recorded below the Salar de Atacama basin (Jordan *et al.*, 2002), with average thicknesses of 0.2 km over an area of 3,000 km² (Jordan *et al.*, 2002) that yields a volume of 600 km³. Nonetheless, a conservative estimate is that the ignimbrites are present below 1/2 and 2/3 of the Salar de Atacama basin, thus reducing the volume to ~300-400 km³. Therefore, the caldera outflow is ~555-655 km³. The final volume of the caldera infill and outflow resulting from these estimates is ~3,400-3,500 km³, larger than by Lindsay *et al.* (2001a) and de Silva and Gosnold (2007) for the combined Pujsa, Toconao and Atana ignimbrites (~2,800 km³). Thus, the resulting volume of the PC and PS calderas makes them some of the largest in the world, comparable to Yellowstone, Toba and La Garita (Mason *et al.*, 2004). Assuming a vesicularity of 35% (Lindsay *et al.*, 2001a), the ignimbrites DRE (dense rock equivalent) is ~2,200-2,300 km³.

The associated VEI is calculated with a modification of the the original scale by Newhall and Self (1982), VEI = $\log_{10}(m)-7$ (Pyle, 1995), with m the mass in kg of the caldera ignimbrites. The mass of the outflow and the caldera infill is ~1.02-$1.05*10^{15}$, thus yielding an average VEI for both ignimbrites of ~8, a figure slightly smaller than the Mason *et al.* (2004) calculation for the Atana eruption, but anyway one of the largest in the world. We note that Mason *et al.* (2004) interpreted their VEI as being produced by the single eruption of Atana ignimbrite, while our calculation considers all the erupted products regardless of the eruption. This discrepancy can also be explained by the smaller density values used in this work (1,900 kg/m³) while Mason *et al.* (2004) used larger values (2,200 - 2,400 kg/m³), thus yielding different estimates. Regardless of the erupted mass and VEI the caldera set considered as a single body (as we cannot discriminate the volumes of La Pacana southern and northern parts) follows the linear logarithmic trend that the larger the caldera radius, the larger the mass deficiency (mass of the erupted volume) (Fig. 6).
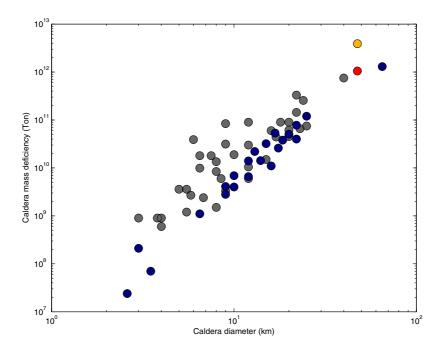

FIG. 6. Comparison of caldera diameter and mass deficiency. Blue circles are data from Campos-Enríquez *et al.* (2005) and Yokoyama (1987). Grey circles are caldera erupted volumes converted to mass deficiency with a density contrast of 300 kg/m³ (Acocella, 2007). Red and yellow circles are La Pacana caldera with the mass deficiency calculated by means of Gauss's theorem and from Mason *et al.* (2004). La Pacana radius was calculated as the mean of the north-south and east-west diameters (Gardeweg and Ramírez, 1987).

6. Conclusions

Despite the low spatial resolution of the gravity data set, first order inferences can be made about the inner structure of the La Pacana caldera that can be compared to different geological interpretations based on previous work. Our reinterpretation of the caldera stratigraphy led us to speculate that its southern part was produced by a different eruption and collapse than its northern zone, therefore La Pacana might be made up of two nested smaller calderas. The modeled maximum intracaldera ignimbrite thicknesses are 0.6-1.1 km and 2.5-3 km for the northern and southern parts that collapsed with downsag and trap-door geometries, different than previous models but more consistent with Gardeweg and Ramírez (1987) than Lindsay *et al*. (2001a) proposals. The average erupted volume of La Pacana is ~3,400-3,500 km^3 (VEI=8) for the combined eruptions, in agreement with models that show that the larger the caldera area, the larger the erupted volume. Further work that will help to better understand the caldera dynamics and clarify its evolution include detailed geochronological work, and denser geophysical surveys that incorporate gravity, aeromagnetic and magnetotelluric data.

Acknowledgements

References

Acocella, V. 2007. Understanding caldera structure and development: an overview of analogue models compared to natural calderas. Earth-Science Reviews 85 (3-4): 125-160.

Battaglia, M.; Roberts, C.; Segall, P. 1999. Magma intrusion beneath Long Valley caldera confirmed by temporal changes in gravity. Science 285 (5436): 2119-2122.

Bahlburg, H.; Breitkreuz, C.; Zeil, W. 1988. Geology of the Coquena Formation (Arenigian-Llanvirnian) in the NW Argentine Puna: constraints on geodynamic interpretation. *In* The Southern Central Andes: contributions to structure and evolution of an active continental margin (Bahlburg, H.; Breitkreuz, C.; Giese, P.; editors), Springer: 71-86. Berlin.

Blakely, R. 1996. Potential theory in gravity and magnetic applications. Cambridge University Press: 441 p. Cambridge.

Breitkreuz, C.; Zeil, W. 1994. The Late Carboniferous to Triassic volcanic belt in Northern Chile. *In* Tectonic of the Southern Central Andes (Reuter, K.J.; Scheuber, E.; Wigger, P.J.; editors). Springer: 277-292. Berlin.

Briggs, I.C. 1974. Machine contouring using minimum curvature. Geophysics 39 (1): 39-48.

Cady, J.W. 1980. Calculation of gravity and magnetic anomalies of finite-length right polygonal prisms. Geophysics 45 (10): 1507-1512.

Campos-Enríquez, J.O.; Domínguez-Méndez, F.; Lozada-Zumaeta, M.; Morales-Rodríguez, H.F.; Andaverde-Arredondo, J.A. 2005. Application of the Gauss theorem to the study of silicic calderas: The calderas of La Primavera, Los Azufres, and Los Humeros (Mexico). Journal of Volcanology and Geothermal Research 147 (1-2): 39-67.

Carle, S.F. 1988. Three-dimensional gravity modeling of the geologic structure of Long Valley caldera. Journal of Geophysical Research 93 (B11): 13237-13250.

Chmielowski, J.; Zandt, G.; Haberland, C. 1999. The Central Andean Altiplano-Puna magma body. Geophysical Research Letters 26 (6): 783-786.

Cole, J.W.; Milner, D.M.; Spinks, K.D. 2005. Caldera and caldera structures: a review. Earth-Science Reviews 69 (1-2): 1-26.

Comeau, M.J.; Unsworth, M.J.; Ticona, F.; Sunagua, M. 2015. Magnetotelluric images of magma distribution beneath Volcán Uturuncu, Bolivia: Implications for magma dynamics. Geology 43 (3): 243-246.

Davy, B.; Caldwell, T. 1998. Gravity, magnetic and seismic surveys of the caldera complex, Lake Taupo, North Island, New Zealand. Journal of Volcanology and Geothermal Research 81 (1-2): 69-89.

DeNosaquo, K.B.; Smith, R.B.; Lowry, A.R. 2009. Density and lithospheric strength models of the Yellowstone-Snake River Plain volcanic system from gravity and

heat flow data. Journal of Volcanology and Geothermal Research 188 (1-3): 108-127.

De Silva, S.L. 1989a. Altiplano-Puna Volcanic Complex of the Central Andes. Geology 17 (12): 1102-1106.

De Silva, S.L. 1989b. Geochronology and stratigraphy of the ignimbrites from the 21º30' S to 23º30' S portion of the Central Andes of northern Chile. Journal of Volcanology and Geothermal Research 37 (2): 93-131.

De Silva, S.L.; Zandt, G.; Trumbull, R.; Viramonte, J.G.; Salas, G.; Jiménez, N. 2006. Large ignimbrite eruptions and volcanotectonic depressions in the Central Andes a thermomechanical perspective. *In* Mechanisms of activity and unrests at large calderas (De Natale, G.; Troise, C.; Kilburn, C.; editors). Geological Society 269: 47-63. London.

De Silva, S.L.; Gosnold, W.D. 2007. Episodic construction of batholiths: Insights from the spatiotemporal development of an ignimbrite flare-up. Journal of Volcanology and Geothermal Research 167 (1-4): 320-335.

Del Potro, R.; Díez, M.; Blundy, J.; Camacho, A.G.; Gottsmann, J. 2013. Diapiric ascent of silicic magma beneath the Bolivian Altiplano. Geophysical Research Letters 40: 2044-2048.

Drenth, B.J.; Keller, G.R.; Thompson, R.A. 2012. Geophysical study of the San Juan Mountains batholith complex, southwestern Colorado. Geosphere 8 (3): 669-684.

Farr, T.G.; Rosen, P.A.; Caro, E.; Crippen, R.; Duren, R.; Hensley, S.; Kobrick, M.; Paller, M.; Rodríguez, E.; Roth, L.; Seal, D.; Shaffer, S.; Shimada, J.; Umland, J.; Werner, M.; Oskin, M.; Burbank, D.; Alsford, D. 2007. The Shuttle Radar Topography Mission. Reviews of Geophysics 45: RG2004.

Gabalda, G.; Bonvalot, S.; Hipkin, R. 2003. CG3TOOL: an interactive computer program to process Scintrex CG-3/3Mgravity data for high-resolution applications. Computers & Geosciences 29 (2): 155-171.

Gardeweg, M.; Ramírez, C. 1985. Hoja Río Zapaleri, II Región de Antofagasta. Servicio Nacional de Geología y Minería, Carta Geologica de Chile, Serie Geología Básica 66: 89 p., 1 mapa 1:250.000. Santiago.

Gardeweg, M.; Ramírez, C. 1987. La Pacana caldera and the Atana ignimbrite -a major ash-flow and resurgent caldera complex in the Andes of northern Chile. Bulletin of Volcanology 49 (3): 547-566.

Gardeweg, M.; Lindsay, J. 2004. Lascar volcano and La Pacana caldera. *In* Proceedings of the IAVCEI General Assembly, Field Trip Guide A2: 32 p. Pucón.

González, G.; Cembrano, J.; Aron, F.; Veloso, E.E.; Shyu, J.B.H. 2009. Coeval compressional deformation and volcanism in the central Andes, case studies from northern Chile (23°S-24°S). Tectonics 28: TC6003.

Götze, H.-J.; Krause, S. 2002. The Central Andean gravity high, a relic of an old subduction complex? Journal of South American Earth Sciences 14 (8): 799-811.

Gudmundsson, M.T.; Högnadóttir, T. 2007. Volcanic systems and calderas in the Vatnajökull region, central Iceland: Constraints on crustal structure from gravity data. Journal of Geodynamics 43 (1): 153-169.

Gupta, V.K.; Ramani, N. 1980. Some aspects of regional-residual separation of gravity anomalies in a Precambrian terrain. Geophysics 45 (9): 1412-1426.

Hammer, S. 1939. Terrain corrections for gravimeter surveys. Geophysics 4 (3): 184-194.

Hammer, S. 1945. Estimating ore masses in gravity prospecting. Geophysics 10 (1): 50-62.

Hardy, S. 2008. Structural evolution of calderas: Insights from two-dimensional discrete element simulations. Geology 36 (12): 927-930.

Holohan, E.P.; Troll, V.R.; Walter, T.R.; Münn, S.; McDonnell, S.; Shipton, Z.K. 2005. Elliptical calderas in active tectonic settings: an experimental approach. Journal of Volcanology and Geothermal Research 144 (1-4): 119-136.

Jones, M.T.; Sparks, R.S.J.; Valdés, P.J. 2007. The climatic impact of supervolcanic ash blankets. Climate Dynamics 29 (6): 553-564.

Jordan, T.E.; Muñoz, N.; Hein, M.; Lowenstein, T.; Godfrey, L.; Yu, J. 2002. Active faulting and folding without topographic expression in an evaporite basin, Chile. Geological Society of America Bulletin 114 (11): 1406-1421.

Kane, M.F. 1962. A comprehensive system of terrain corrections using a digital computer. Geophysics 27 (4): 455-462.

LaFehr, T.R. 1965. The estimation of the total amount of anomalous mass by Gauss' theorem. Journal of Geophysical Research 70 (8): 1911-1919.

LaFehr, T.R. 1991a. Standardization in gravity reduction. Geophysics 56 (8): 1170-1178.

LaFehr, T.R. 1991b. An exact solution for the gravity curvature (Bullard B) correction. Geophysics 56 (8): 1179-1184.

Lindsay, J.M. 1999. Stratigraphy, age relations and magmatic evolution of large-volume felsic ignimbrites of the La Pacana Caldera, Central Andes, Chile. Ph.D. Thesis (Unpublished), GeoForschungsZentrum Potsdam: 141 p.

Lindsay, J.M.; de Silva, S.; Trumbull, R.; Emmermann, R.; Wemmer, K. 2001a. La Pacana caldera, N. Chile: a re-evaluation of the stratigraphy and volcanology of

one of the world's largest resurgent calderas. Journal of Volcanology and Geothermal Research 106 (1-2): 145-173.

Lindsay, J.M.; Schmitt, A.K.; Trumbull, R.B.; De Silva, S.L.; Siebel, W.; Emmermann, R. 2001b. Magmatic evolution of the La Pacana caldera system, central Andes, Chile: compositional variation of two cogenetic, large-volume felsic ignimbrites and implications for contrasting eruption mechanisms. Journal of Petrology 42 (3): 459-486.

Lipman, P.W. 1997. Subsidence of ash-flow calderas: relation to caldera size and magma-chamber geometry. Bulletin of Volcanology 59 (3): 198-218.

Lipman, P.W. 2007. Incremental assembly and prolonged consolidation of Cordilleran magma chambers: Evidence from the Southern Rocky Mountain volcanic field. Geosphere 3 (1): 42-70.

Longman, I.M. 1959. Formulas for computing the tidal accelerations due to the moon and the sun. Journal of Geophysical Research 64 (2): 2351-2355.

Martí, J.; Geyer, A.; Folch, A.; Gottsmann, J. 2008. A review on collapse caldera modelling. *In* Caldera Volcanism: Analysis, Modeling and Response (Gottsmann, J.; Martí, J.; editors). Elsevier 6: 233-283. Amsterdam.

Malengreau, B.; Lénat, J.-F.; Froger, J.-L. 1999. Structure of Réunion Island (Indian Ocean) inferred from the interpretation of gravity anomalies. Journal of Volcanology and Geothermal Research 88 (3): 131-146.

Mason, B.G.; Pyle, D.M.; Oppenheimer, C. 2004. The size and frequency of the largest explosive eruptions on Earth. Bulletin of Volcanology 66 (8): 735-748.

Masturyono; McCaffrey, R.; Wark, A.; Roecker, S.W.; Fauzi; Ibrahim, G.; Sukhyar, 2001. Distribution of magma beneath Toba caldera, north Sumatra, Indonesia, constrained by 3-dimensional P-wave velocities, seismicity, and gravity data. Geochemistry Geophysics Geosystems 2 (4): (1014). doi: 10.1029/2000GC000096.

Miller, C.; Wark, D. 2008. Supervolcanoes and their explosive supereruptions. Elements 4 (1): 11-16.

Morelli, C.; Gantar, C.; Honkasalo, T.; McConnell, R.K.; Tanner, J.G.; Szabo, B.; Uotila, U.; Whalen, C.T. 1974. The International Standardization Network 1971 (IGSN71). Bulletin Géodésique, Special Publication No. 4. Paris.

Moritz, H. 1984. Geodetic Reference System 1980. Bulletin Géodésique 58 (3): 388-398.

Nagy, D. 1966. The gravitational attraction of a right rectangular prism. Geophysics 31 (2): 362-371.

Newhall, C.G.; Self, S. 1982. The Volcanic Explosivity Index (VEI): an estimate of explosive magnitude for historical volcanism. Journal of Geophysical Research 87 (C2): 1231-1238.

Nettleton, L.L. 1939. Determination of density for reduction of gravimeter observations. Geophysics 4 (3): 176-183.

Parasnis, D.S. 1962. Principles of Applied Geophysics. Methuen: 176 p. London.

Pavez, A. 2005. Structure et déformations du Volcan Lascar à partir d'observations par satellites et au sol: Apports à la connaissance et la surveillance de volcans andésitiques. Ph.D. Thesis (Unpublished), Institut de Physique du Globe de Paris: 381 p.

Pavez, A.; Cortés, J.A.; Self, S.; Kuwata, A.K.; Gardeweg, M. 2008. New insights on La Pacana caldera system, northern Chile, and its ignimbrite sheets. *In* Proceedings of the IAVCEI General Assembly: p 72. Reykjavik.

Pyle, D. 1995. Mass and energy budgets of explosive volcanic eruptions. Geophysical Research Letters 22 (5): 563-566.

Ramírez, C.F.; Gardeweg, M. 1982. Geología de la Hoja Toconao, Región de Antofagasta. Servicio Nacional de Geología y Minería, Carta Geológica de Chile, Serie Geología Básica 54: 117 p., 1 mapa 1:250.000. Santiago.

Ramelow, J.; Riller, U.; Romer, R.L.; Oncken, O. 2006. Kinematic link between episodic trapdoor collapse of the Negra Muerta caldera and motion on the Olacapato-El Toro fault zone, southern central Andes. International Journal of Earth Science 95 (3): 529-541.

Riller, U.; Petrinovic, I.; Ramelow, J.; Strecker, M.; Oncken, O. 2001. Late Cenozoic tectonism, collapse caldera and plateau formation in the central Andes. Earth and Planetary Science Letters 188 (3-4): 299-311.

Riller, U.; Götze, H.-J.; Schmidt, S.; Trumbull, R.B.; Hongn, F.; Petrinovic, I.A. 2006. Upper-crustal structure of the Central Andes inferred from dip curvature analysis of isostatic residual gravity. In The Andes, Active Subduction Orogeny (Oncken, O.; Chong, G.; Franz, G.; Giese, P.; Götze, H.-J.; Ramos, V.A.; Strecker, M.R.; Wigger, P.; editors). Springer 15: 327-336. Berlin.

Rowland, J.V.; Wilson, C.J.N.; Gravley, D.M. 2010. Spatial and temporal variations in magma-assisted rifting, Taupo Volcanic Zone, New Zealand. Journal of Volcanology and Geothermal Research 190 (1-2): 89-108.

Roy, A. 1962. Ambiguity in geophysical interpretation. Geophysics 27 (1): 90-99.

Rymer, H.; Brown, G.C. 1986. Gravity fields and the interpretation of volcanic structures; geological discrimination and temporal evolution. Journal of Volcanology and Geothermal Research 27 (3-4): 229-254.

Salisbury, M.J.; Jicha, B.R.; De Silva, S.L.; Singer, B.S.; Jiménez, N.C.; Ort, M.H. 2011. [40]Ar/[39]Ar chronostrati-

graphy of Altiplano-Puna volcanic complex ignimbrites reveals the development of a major magmatic province. Geological Society of America Bulletin 123 (5-6): 821-840.

Seebeck, H.; Nicol, A.; Stern, T.A.; Bibby, H.M.; Stagpoole, V. 2009. Fault controls on the geometry and location of the Okataina Caldera, Taupo Volcanic Zone, New Zealand. Journal of Volcanology and Geothermal Research 190 (1-2): 136-151.

Self, S. 2006. The effects and consequences of very large explosive volcanic eruptions. Philosophical Transactions of the Royal Society 364 (1845): 2073-2097.

Self, S.; Blake, S. 2008. Consequences of explosive supereuptions. Elements 4 (1): 41-46.

Schilling, F.R.; Trumbull, R.B.; Brasse, H.; Haberland, C.; Asch, G.; Bruhn, D.; Mai, K.; Haak, V.; Giese, P.; Muñoz, M.; Ramelow, J.; Rietbrock, A.; Ricaldi, E.; Vietor, T. 2006. Partial Melting in the Central Andean Crust: a Review of Geophysical, Petrophysical, and Petrologic Evidence. *In* The Andes, Active Subduction Orogeny (Oncken, O.; Chong, G.; Franz, G.; Giese, P.; Götze, H.-J.; Ramos, V.A.; Strecker, M.R.; Wigger, P.; editors). Springer 22: 459-474. Berlin.

Schmidt, S.; Götze, H.-J. 2006. Bouguer and isostatic maps of the Central Andes. *In* The Andes, Active Subduction Orogeny (Oncken, O.; Chong, G.; Franz, G.; Giese, P.; Götze, H.-J.; Ramos, V.A.; Strecker, M.R.; Wigger, P.; editors). Springer 28: 559-562. Berlin.

Schmitt, A.K.; Lindsay, J.M.; De Silva, S.L.; Trumbull, R.B. 2002 U-Pb zircon chronostratigraphy of early-Pliocene ignimbrites from La Pacana, north Chile: implications for the formation of stratified magma chambers. Journal of Volcanology and Geothermal Research 120 (1-2): 43-53.

Simons, M.; Galetzka, J.E.; Genrich, J.F.; Ortega, F.; Comte, D.; Glass, B.; González, G. 2010. Central Andean Tectonic Observatory Geodetic Array: CJNT-Chajnantor P.S., UNAVCO, GPS Data Set. doi :10.7283/T5B27S9T.

Simpson, R.W.; Jachens, R.C.; Blakely, R.; Saltus, R.W. 1986. A new isostatic residual gravity map of the conterminous United States with a discussion on the significance of isostatic residual anomalies. Journal of Geophysical Research 91 (B8): 8348-8372.

Smith, N.; Cassidy, J.; Locke, C.A.; Mauk, J.L.; Christie, A.B. 2006. The role of regional-scale faults in control-

ling a trapdoor caldera, Coromandel Peninsula, New Zealand. Journal of Volcanology and Geothermal Research 149 (3-4): 312-328.

Sparks, S.; Self, S.; Grattan, J.; Oppenheimer, C.; Pyle, D.; Rymer, H. 2005. Super eruptions, global effects and future threats. Report of a Geological Society of London Working Group, 25 p. https://www.geolsoc.org.uk/Education-and-Careers/Resources/Papers-and-Reports/Super-eruptions (last visit 31-08-2015)

Tassara, A.; Götze, H.-J.; Schmidt, S.; Hackney, R. 2006. Three-dimensional density model of the Nazca plate and the Andean continental margin. Journal of Geophysical Research 111: B09404.

Telford, W.M.; Geldart, L.P.; Sheriff, R.E. 1990. Applied Geophysics. Cambridge University Press: 770 p. Cambridge

Tiede, C.; Camacho, A.G.; Gerstenecker, C.; Fernández, J.; Suyanto, I. 2005. Modeling the density at Merapi volcano area, Indonesia, via the inverse gravimetric problem. Geochemistry Geophysics Geosystems 6: Q09011.

Torge, W. 1989. Gravimetry de Gruyter: 465 p. New York.

Yokoyama, I. 1987. A quantitative consideration of several calderas for study of their formation. Geofísica Internacional 26 (4): 487-498.

Ward, K.M.; Zandt, G.; Beck, S.L.; Christensen, D.H.; McFarlin, H. 2014. Seismic imaging of the magmatic underpinnings beneath the Altiplano-Puna volcanic complex from the joint inversion of surface wave dispersion and receiver functions. Earth and Planetary Science Letters 404: 43-53.

Wessel, P.; Smith, W.H.F. 1998. New improved version of the Generic Mapping Tools released. Eos, Transactions American Geophysical Union 79 (47): p. 579.

Wicks, C.W.; Thatcher, W.; Dzurisin, D.; Svarc, J. 2006. Uplift, thermal unrest and magma intrusion at Yellowstone caldera. Nature 440: 72-75.

Wilson, C. 2008. Super eruptions and supervolcanoes: processes and products. Elements 4 (1): 29-34.

Zandt, G.; Leidig, M.; Chmielowski, J.; Baumont, D.; Yuan, X. 2003. Seismic detection and characterization of the Altiplano-Puna magma body, Central Andes. Pure and Applied Geophysics 160 (3-4): 789-807.